

Crack self-healing behavior in silicon carbide composite ceramics to secure structural integrity and improve economics

Pete Sihyun Lee^a, Tae-Ho Ahn^b, Sung-Hun Kim^c, Hyun-Mi Kim^c and Kwang-Bo Shim^{b,*}

^aMorgan Advanced Materials, 394, Dunchon-daero, Jungwon-gu, Seongnam-si, Gyeonggi-do, Korea

^bInternational Sustainable Engineering Materials (ISEM) Center, Ceramic Materials Institute, Hanyang University, Seoul 133-791 Korea

^cDivision of Materials Science and Engineering, 222 Wangsimni-ro, Seongdong-gu, Hanyang University, Seoul 133-791 Korea

Structural ceramics are brittle and sensitive to flaws. As a result, the structural integrity of ceramic component may be seriously affected. However some engineering ceramics have the ability to healing the crack that is considerable advantages can be expected. In this review, the structural ceramics and its structure, parts processing and physical properties in terms of commercial products that are using today. Crack-healing behavior and mechanism was investigated in different silicon carbide based materials; alumina, mullite, silicon nitride, aluminum nitride, and zirconium debride. To find self-healing conditions in economical way for commercial structural ceramics, self-healing parameters are reviewed based on silicon carbide composite ceramics; healing temperature, testing temperature, healing atmosphere, crack size, SiC volume fraction, applied healing and testing stress, threshold stress for crack-healing, and fatigue stress. It can be conclude that crack-healing is effective way to increase reliability and lifetime of ceramics, and cost can be dramatically reduced by reducing quality inspection cost and time. Enhancing the self-crack-healing ability is valuable way to expand the usage of SiC ceramics such as engineering parts in extremely hard conditions and advanced semiconductor parts for higher density of circuit.

Key words: Self-healing, Crack-healing, Silicon carbide, Silicon nitride, Aluminum nitride, Mullite.

Introduction

Ceramics are candidate materials for industrial applications because of their excellent mechanical, tribological and thermal properties. Structural ceramics has heat-resistant limit that is 1273 K-1773 K, which is greatly superior to that of metallic material[1]. These features have applications include bearings, turbo charger rotors, diesel engine components and cutting tools. However, because ceramics are brittle materials, fracture toughness is lower than that of metallic materials, resulting in lower reliability in mechanical properties. Thus, if the brittleness of ceramics is overcome, the reliability and product life of ceramic components will be improved. Many studies have been carried out to overcome the low fracture toughness of ceramics by (a) toughening the ceramic by fiber or whisker reinforcement, and microstructure control and (b) activating the crack-healing ability to heal surface cracks introduced during machining and service. Some structural ceramics have a self-crack-healing ability. If this ability is used on ceramic components, great merits can be anticipated in the following areas: (a) an increase in reliability (b) decreases in inspection, machining and polishing costs, and (c) decreases in

maintenance costs and prolongation of the lifetime of the ceramic [2].

Silicon carbide (SiC) ceramics has unique properties in combination with other ceramics such as alumina, silicon nitride, mullite, and zirconia as a multi composite. Silicon carbide ceramics find extensive application in several fields of engineering as materials for advanced energy systems, such as high performance combustion systems, fuel-flexible gasification systems, fuel cell/turbine hybrid systems, nuclear fusion reactors and high temperature gas-cooled fission reactors.

Silicon carbide parts global market which includes monolith and ceramic matrix composite reaches 3 billion USD dollars and growing with semiconductor industry. Single crystal SiC is promising material for high voltage and frequency power semiconductor device replacing silicon wafer. Silicon carbide parts are manufacturing with many different ways to decide performance and economics. The structural ceramics property was reviewed, focusing on silicon carbide in terms of mechanical, thermal, chemical and electrical. To know the commercial products helps to resolve its flaws.

Many authors have researched the crack-healing behavior of structural ceramics, Ando and co-workers, intensively investigated Silicon carbide composite ceramics. Silicon carbide is the key material to get the self-healing ability and generate oxidation mixing with alumina, silicon nitride, mullite, and zirconia. More

*Corresponding author:
Tel : +82-2-2220-0501
Fax: +82-2-2220-7395
E-mail: kbshim@hanyang.ac.kr

than 15 vol% SiC can recover the crack strength completely and they found that healed zone is mechanically stronger than the base material [3-5].

In this paper, crack-healing mechanism was discussed in different composite materials. Pre-crack test and bending strength test results before and after healing investigated in the healing condition; healing temperature, testing temperature, healing atmosphere, crack size, SiC volume fraction, applied healing and testing stress, threshold stress for crack-healing, and fatigue stress. Heat resistance limit is also key features in combination with mechanical strength, which is describing actual usage condition.

Silicon Carbide and Fabrication

Silicon carbide

Silicon carbide is considered one of the few lightweight covalently bonded ceramics. The structure of SiC is shown in Fig. 1 [6]. It can be seen that SiC is the only compound of silicon and carbon to occur in the condensed state in addition to elemental silicon and carbon. The theoretical density of β -SiC is only 3.210 g/cm³ and that of α -SiC (6H polytype) is 3.208 g/cm³. Combining its lightweight and, strong covalency with other properties, such as low thermal expansion coefficient and high thermal conductivity, strength and hardness, make SiC a promising ceramic for the replacement of conventional metals, alloys and ionic bonded ceramic oxides.

Since the late 19th century silicon carbide has been an important material for sandpapers, grinding wheels, and cutting tools. More recently, it has found application in refractory linings and heating elements for industrial furnaces, in wear-resistant parts for pumps and rocket engines, and in semiconducting substrates for light-emitting diodes.

There are numerous (~ 200) polytypes for SiC, but only a few are common. All of the structures may be visualized as being made up of a single basic unit, a layer of tetrahedra, in which each silicon atom is tetrahedrally bonded to four carbon atoms and each carbon atom is tetrahedrally bonded to four silicon atoms. The differences among the existing polytypes

are the orientational sequences by which such layers of tetrahedra are stacked. Successive layers of tetrahedra may be stacked in only one of two ways or orientations but with many possible sequential combinations, each of which represent a different crystal polytype.

Fabrication

The most common forms of SiC include powders, fibers, whiskers, coatings and single crystals. There are several methods to produce SiC depending on the product form desired and its application. Purity of the product imposes certain restrictions on the selection of the method of production.

Ceramic materials that demonstrate enhanced mechanical properties under demanding conditions. Because they serve as structural members, often being subjected to mechanical loading, they are given the name structural ceramics. Ordinarily, for structural applications ceramics tend to be expensive replacements for other materials, such as metals, polymers, and composites. Advanced structural ceramics are in production for wear parts, cutting tools, bearings, filters, and coatings. Table 1 shows some current and future application of structural ceramics.

The production of most ceramics, including both traditional and advanced ceramics, consists of the following process steps: powder preparation, forming, densification, and finishing. The most important processing techniques involved in the steps are identified in table 2. Finishing step involves such processes as grinding and machining with diamond and boron nitride tools, chemical etching, and laser and electric discharge machining.

The high hardness and chemical inertness of Silicon Carbide ceramics make the finishing operations some of the most difficult and expensive in the entire process. Grinding alone can account for a large fraction of the cost of the component. In addition, surface cracks are often introduced during machining, and these can reduce the strength of the part and the yields of the fabrication process.

Self-healing Experiment

Mechanical strength test

The flexural strength is defined as a measure of the ultimate strength of a specified beam in bending. The beam is subjected to a load at a steady rate until rupture takes place. If the material is ductile, like most metals and alloys, the material bends prior to failure. On the other hand, if the material is brittle, such as ceramics and graphite, there would be a very slight bending followed by a catastrophic failure. There are two standard tests to determine the flexural strength of materials: the four-point test shown in Fig. 2 [7] and the three-point test in Fig. 3 [8]. In the four-point test, the specimen is symmetrically loaded at two locations that are situated one quarter of the overall span

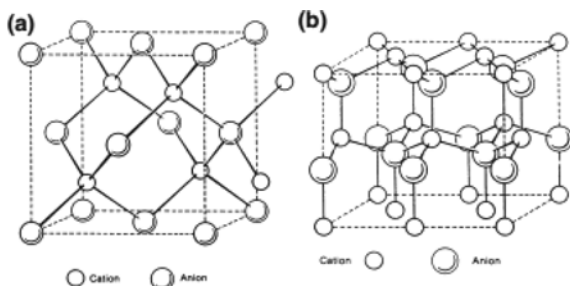


Fig. 1. SiC Crystal Structures: (a) Zinc Blend Structure for β -SiC and (b) Wurtzite Structure for 6H α -SiC. From [8].

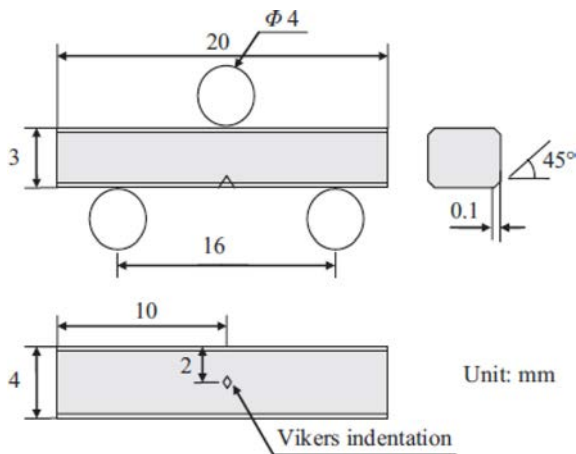


Fig. 2. Three-point bending test, From [12].

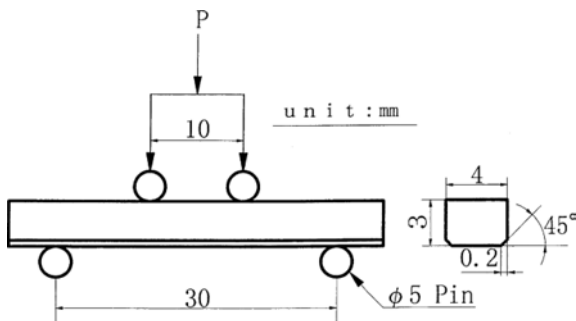


Fig. 3. Four-point bending test, From [13].

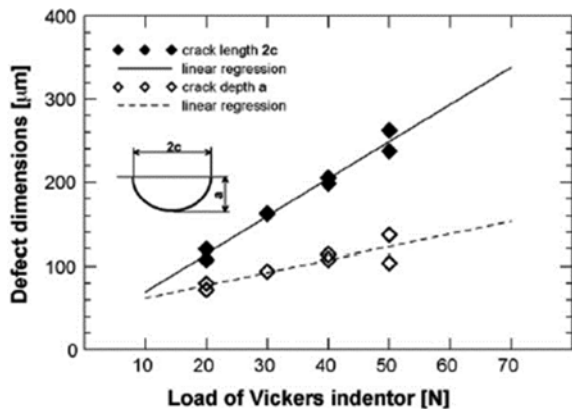


Fig. 4. Indicative dimensions of the crack caused by application of different load during Vickers indentation, From [9].

between two support spans. In the three-point test, the load is applied at the middle of the specimen between two support bearings. However the test results, bending strength are different. As shown in Table 3, as an example of commercial CVD SiC product, four-point gives 450 Mpa, three-point tells higher than four-point that is 560 Mpa at 1300 °C [9].

Pre-crack generation

To investigate the crack healing behavior of the specimens with a semi-elliptic surface crack produced by the Vickers indentation in the middle of the beam at

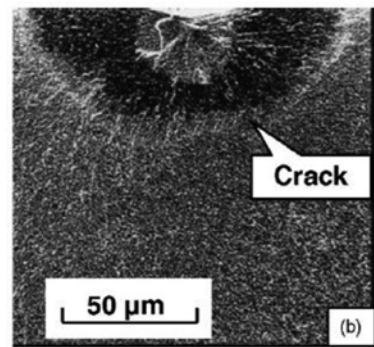
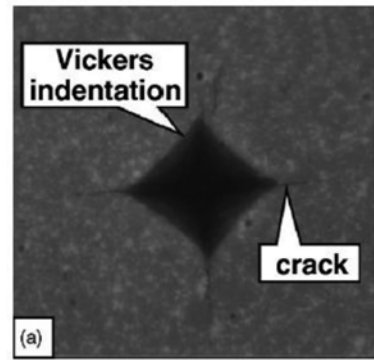


Fig. 5. SEM images of (a) indented crack and (b) crack shape. From [10].

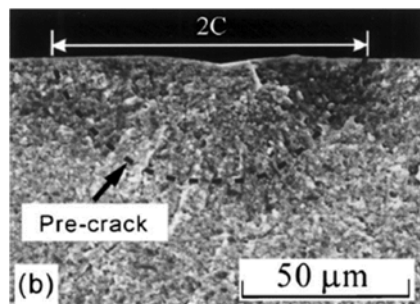
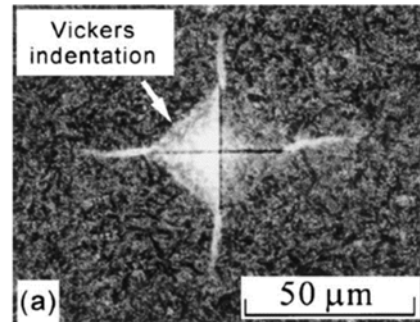


Fig. 6. SEM photographs of (a) Vickers indented crack on the surface and (b) crack surface, From [11].

a different load of 10 N, 20 N, 30 N, 40 N, 50 N were applied in Fig 4 [3]. As increasing the load, the crack length and depth is linearly increasing.

The indentation and crack length are shown in Fig. 5(a) [3]. Crack shapes were confirmed on the fracture surfaces of cracked specimens as shown in Fig. 5(b). Small cracks propagate around the main crack that can be

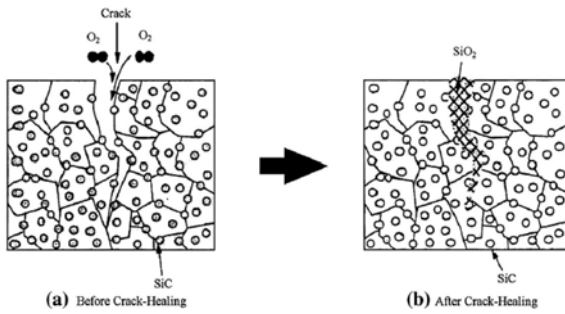


Fig. 7. Schematic diagrams showing crack-healing model.

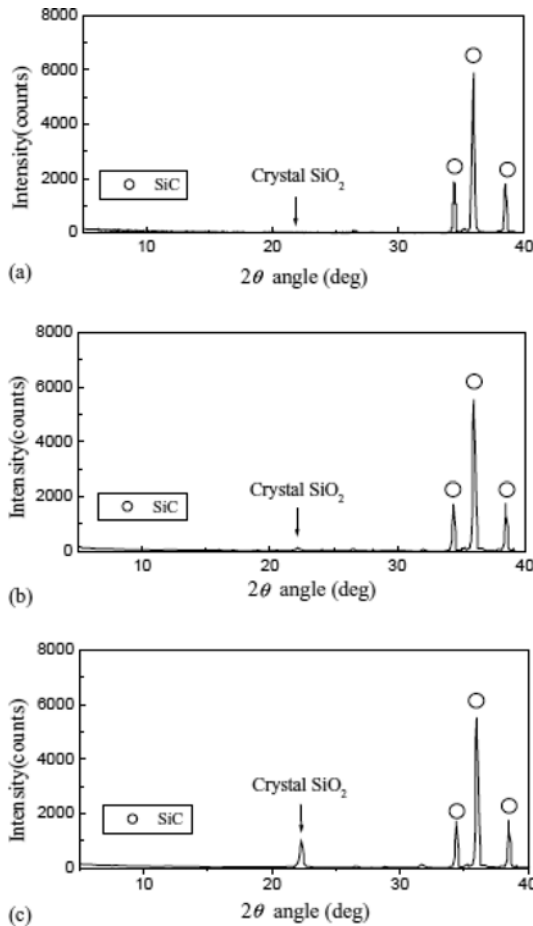


Fig. 8. XRD observation of healing process (a) smooth specimen subjected to no crack-healing treatment, (b) crack-healed at 1773 K, 1 h, (c) crack-healed at 1773 K, 40 h.

grow in the ceramics in Fig. 6 [7].

Crack healing Behavior and Mechanism

Silicon carbide ceramic

To understand the behavior of the crack-healing, the XRD (X-ray Diffraction) analysis and EPMA (Electron Probe Micro Analyzer) observation are applied to the surface oxide of healed specimens [10]. Fig. 7 shows the mechanism of the crack-healing model. When looking at the schematic diagrams, it is assumed that

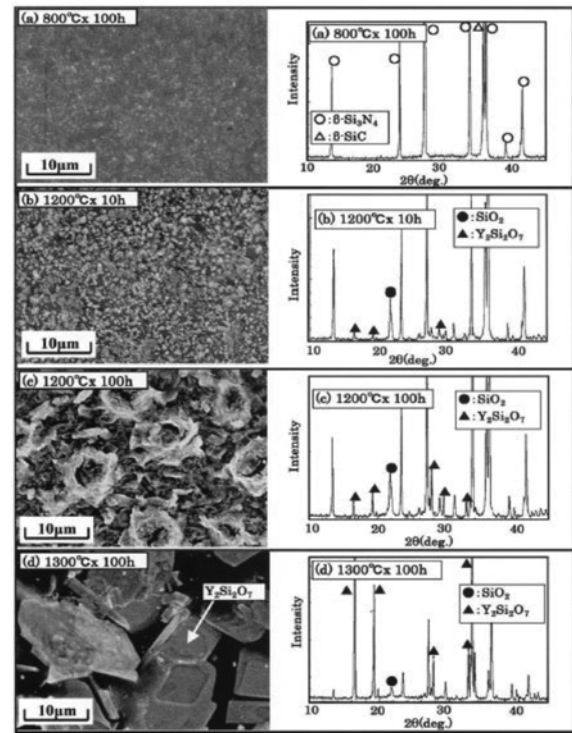


Fig. 9. SEM images and XRD results of healed sample surface: (a) TH = 800 °C, tH = 100 h, (b) TH = 1200 °C, tH = 10 h, (c) TH = 1200 °C, tH = 100 h, (d) TH = 1300 °C, tH = 100 h. From [17].

the crack-healing is due to oxidation. The estimated crack-healing reactions are the following, oxidation and exothermic reaction, where the oxygen that intruded the cracked surface, react on silicon carbide (SiC) that in the cracked surface.



As the results of XRD, large amounts of SiO_2 and a small amount of CO_2 or CO gas are detected, for healing these cracks. As represented in Eq. (1), the production of SiO_2 is a glass phase and crystal phase. At room temperature, even produced in any phase, though the difference of the strength is not large, in the matter that represented by the crystal phase, its heat-resistance limit and high temperature strength are very excellent. On the other hand, in the matter of the crack-healing, how many amount of crystal phase can be precipitated, this is the main technology of crack-healing [11]. As the healing progress, XRD can observe of growing crystal SiO_2 phase according to increase healing time in Fig. 8. [12]

Silicon nitride and silicon carbide composite ceramic

To make a $\text{Si}_3\text{N}_4/\text{SiC}$ composite, Y_2O_3 is used as additive to decrease the sintering temperature and strengthen the structure. As an example of mixing the composite, silicon nitride powder commonly used had a mean particle size of 0.2 μm , and a volume ratio of

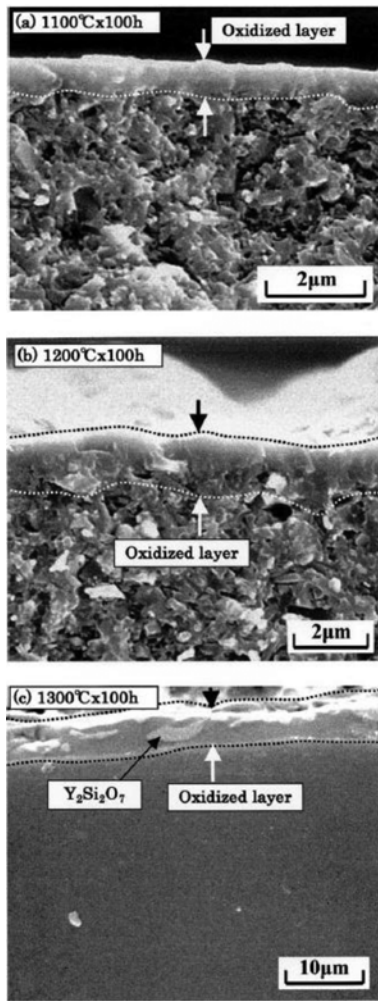


Fig. 10. SEM images of oxidized layer: (a) TH = 1100 °C, tH = 100 h, (b) TH = 1200 °C, tH = 100 h, (c) TH = 1300 °C, tH = 100 h. From [17].

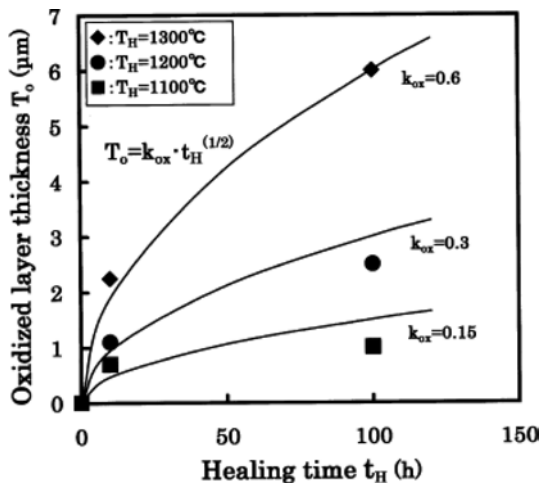


Fig. 11. Relationship between crack-healing time (tH) and thickness of oxidized layer (TO). From [17].

α -Si₃N₄ of 95% (the rest is β -Si₃N₄). The SiC powder used had a mean particle size of 0.03 μm, and the sample contained 18.5% SiC powder. Y₂O₃ 8 wt% was

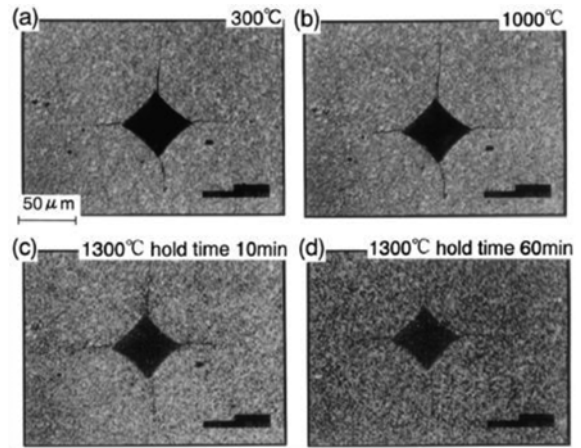


Fig. 12. Observation of the crack-healing process using a laser microscope.

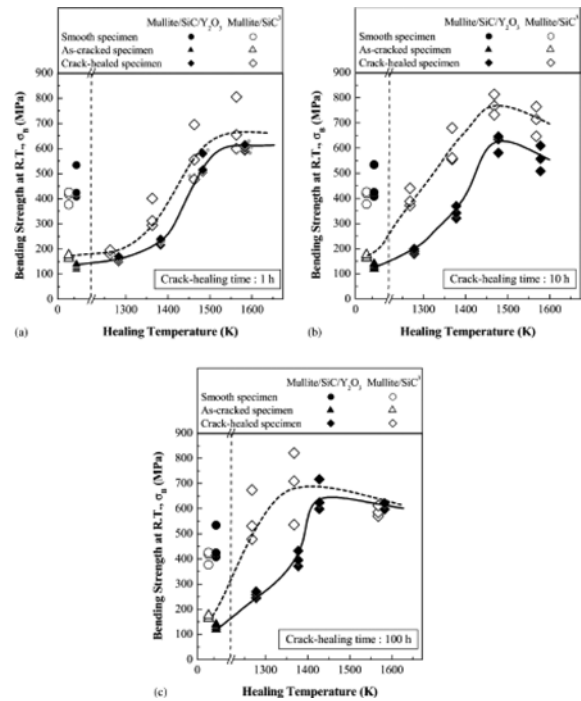
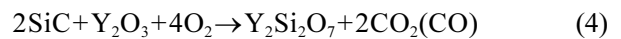
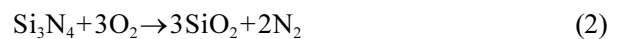


Fig. 13. Relationship between bending strength at room temperature and crack healing temperature. Data marked with an asterisk indicate that fracture occurred outside of the crack-healed zone: (a) crack-healing time: 1 h, (b) crack-healing time: 10 h and (c) crack-healing time: 100 h. From [16].

added to Si₃N₄ powder with SiC powder as a sintering additive. The estimated crack-healing reactions of this sample are following [13].



It is assumed that the crack-healing is due to oxidation. In reactions (3) and (4), gases generated

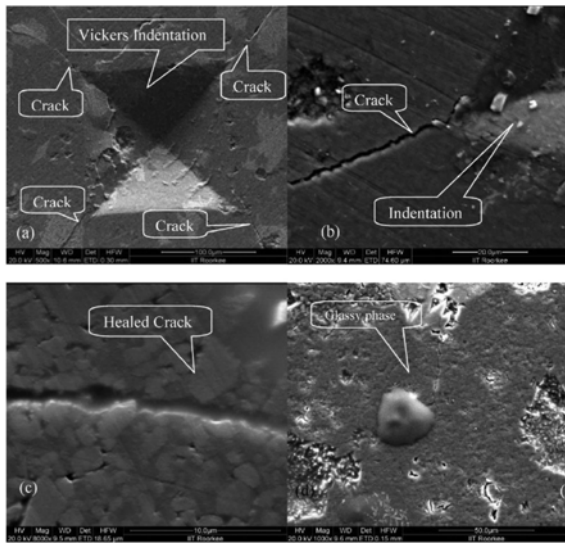
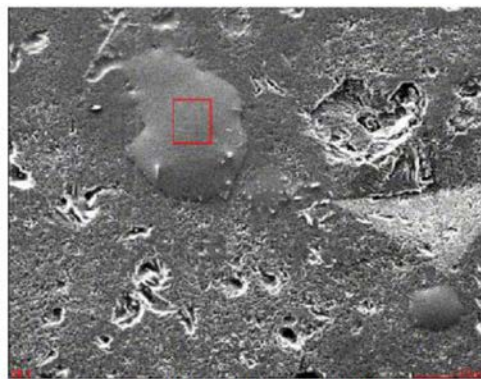


Fig. 14. SEM micrographs of the sample surfaces showing (a) indentation with cracks, (b) crack shape, (c) healed crack after heat treatment and (d) glassy phase formed after heat treatment.



(a)

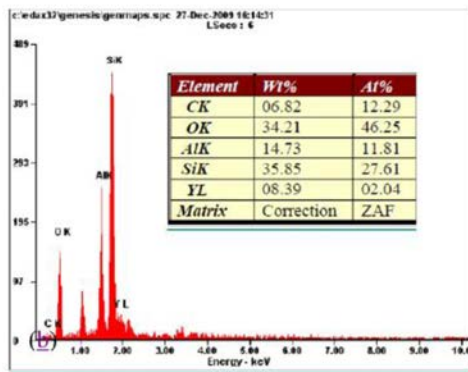


Fig. 15. (a) Micrograph of a healed crack surface showing glassy phase formed and (b) EDS analysis result of the glassy phase through area scan.

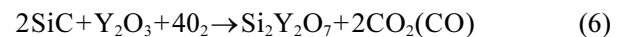
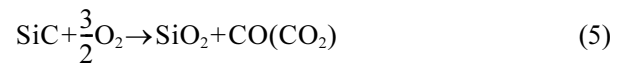
during healing are CO_2 or CO depend on healing temperature. At 1200–1400 °C healing reactions (3) and (4) are dominant and both SiO_2 and $\text{Y}_2\text{Si}_2\text{O}_7$ show a crystal phase, if enough SiC particles are added. However, at 1000 °C, most SiO_2 shows glassy phase, if special healing process is not applied. Surface of

specimens healed in each environment was analyzed with XRD. The only specimen healed in air diffracts the SiO_2 peaks intensely in Fig. 9 [14].

The oxidized layer thickness (T_o) on the sample surfaces were measured, using an SEM, as a function of crack-healing temperature and time, and shown in Fig. 14. Fig. 10(a) shows the T_o on the fracture surface under the condition of $T_H = 1100$ °C, $t_H = 100$ h. The oxidized zone looks like a glassy phase, so it can be distinguished from base material easily. The T_o is almost uniform and about 1 μm in thickness. Fig. 10(b) is the SEM image of the fracture surface, and Fig. 10(c) is the SEM image of the polished surface. The T_o was measured systematically using these SEM images, and the relationship between the healing time (t_H) and oxidized layer thickness (T_o) is shown in Fig. 11. The oxidation behavior of four kinds of Si_3N_4 followed parabolic-law kinetics up to 100 h at 1300 °C. Thus oxidation layer growth has great dependency in healing temperature and time.

Mullite and Silicon Carbide composite ceramic

Monolithic Mullite has no crack-healing capability. However, a large self-crack healing ability was successfully induced in mullite/SiC and mullite/SiC/ Y_2O_3 ceramic. It is known that Y_2O_3 is very useful sintering additive and contribute to healing with oxidation reaction (6) of $\text{Si}_2\text{Y}_2\text{O}_7$. It has been reported that the optimal Y_2O_3 content of mullite is 0.5 mass% and mullite/SiC is 1–2 mass% [19, 34]. The crack-healing is caused by the oxidation reaction as follows [18].



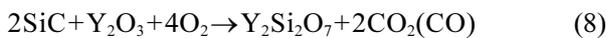
The mullite/SiC composite pre-crack zone was observed directly with a laser microscope during the heat treatment process to investigate the strength recovery. The crack was obvious at 1000 °C in Fig. 12(a) and no changes were observed. However, the crack could not be clearly distinguished 10 min after it reached 1300 °C, as shown in Fig. 12(c). The crack could barely be observed after 1h at 1300 °C because the surface was covered with some newly created phases in Fig. 12(d).

Fig. 13 shows the relationship between bending strength at room temperature and crack-healing temperature. The closed and open symbols indicate the test results of mullite/SiC/ Y_2O_3 and mullite/SiC, respectively, where the SiC content of the mullite/SiC composite is 15 vol.%. The minimum temperatures (T_H) at which the average σ_B of the crack-healed specimen exceeded the average σ_B of the smooth specimens. The crack-healing ability of mullite/SiC/ Y_2O_3 is similar to that of mullite/SiC. However, the average σ_B of mullite/SiC/ Y_2O_3 is lower than that of

mullite/SiC. Nevertheless, most specimens of mullite/SiC/Y₂O₃ crack-healed above minimum crack healing temperature, T_H, fractured from a point outside of the crack-healed zone. Therefore, the σ_B of crack healed mullite/SiC/Y₂O₃ recovered completely, thus the crack healing condition at 1573 K for 1 h in air was determined to be optimal.

Alumina and Silicon carbide composite ceramic

The crack-healing mechanisms of Al₂O₃/SiC composite and Al₂O₃ monolithic were very different. The crack-healing of Al₂O₃/SiC composite is caused by the following chemical reaction [20, 21].



It is assumed that the crack-healing is due to oxidation, where, the oxygen that intrudes the cracked surface reacts with silicon carbide (SiC) present there. The extra bonding force exerted by the glass phase on the crack, either by transfer of the existing glass phase to the crack plane to bridge it [22] or owing to the reaction of the crack surface with the oxidation environment [23] bridges it. However, that of Al₂O₃ monolithic is fully oxidized and more oxidation is impossible, thus, crack-healing is caused by secondary sintering. [24]

A higher heating temperature and longer holding time promote the oxidation reaction of SiC. The oxidation results in silica either in amorphous or cristobalite forms, depending upon the temperature of operation. The amorphous silica, converts into a crystallized cristobalite form, above 1100 °C. Mullitization occurs due to the reaction between Al₂O₃ and the oxidation derived SiO₂ at 1400 °C. However, the presence of Y₂O₃ in Al₂O₃-SiO₂ system lowers the mullitization temperature by about 100 °C. Mullitization is governed by a solution-precipitation control mechanism. The reaction between SiO₂ and Al₂O₃ produces a metastable eutectic liquid to form a transitory aluminosilicate glass, which dissolves alumina giving rise to mullite precipitate. The eutectic compound (liquid) formed in the system Y₂O₃-SiO₂-Al₂O₃ has a low viscosity and therefore is able to flow into the pore channels thereby filling in some pores and cracks with this compound. [25] The evidence of the presence of glassy phase in a healed crack is also demonstrated by EDS analysis as depicted in Fig. 14 and 15.

Aluminum nitride and Silicon carbide composite ceramic

Crack-healing behavior of silicon carbide-aluminum nitride (SiC-AIN) composites is one of the best candidates for high temperature applications among SiC-based materials. SiC-AIN composites were made

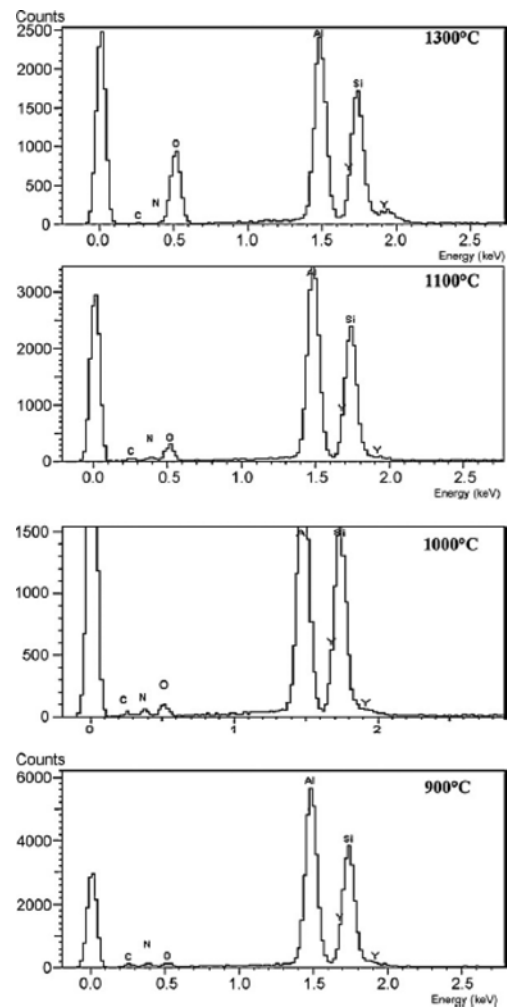


Fig. 16. XRD patterns of the as-sintered and healed (1300 °C, 1h) SiC-AIN specimens.

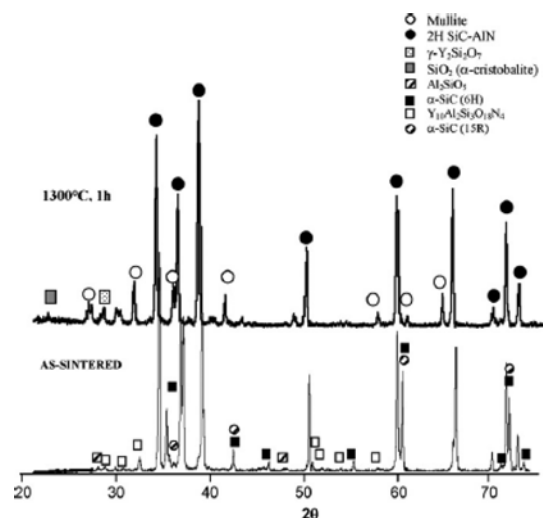
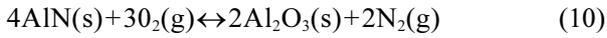
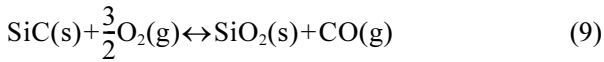


Fig. 17. EDS spectra acquired on the surface of SiC-AIN ceramics after heat treatments in the temperature range 900-1300 °C.

by means of pressureless sintering using Ytria (Y₂O₃) as sintering aid. The possible mechanism of the crack-healing is based on the formation of oxides (cristobalite, mullite) on the basis of the following

reactions:



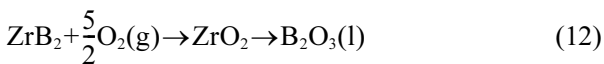
Reactions (9) and (10) are, respectively, the oxidation of silicon carbide (passive oxidation) and aluminum nitride, while reaction (11) leads to the formation of mullite. The XRD spectra reported in Fig. 16 shows that mullite and cristobalite were formed after heat-treatment at 1300 °C. Traces of yttrium disilicate ($\text{Y}_2\text{Si}_2\text{O}_7$) were also detected due to the decomposition of the grain boundary phase $\text{Y}_{10}\text{Al}_2\text{Si}_3\text{O}_{18}\text{N}_4$. [26]

Another confirmation of the mechanism for the crack-healing could be extracted by the analysis of the EDS spectra reported in Fig. 17. In fact, it is clearly shown that the oxygen content increases with the temperature of the heat-treatment as a consequence of the increase of the silica-based oxides content. These crystalline phases filled or healed the surface cracks after heat treatment in air. Analogous mechanism was proposed by Kim *et al.* [27] in liquid-phase sintered silicon carbide (LPS-SiC) where crack healing also made it possible to recover the strength of different LPS-SiC ceramics treated at different temperature.

Zirconium debride and Silicon carbide composite ceramic

As ultrahigh-temperature ceramics (UHTCs), zirconium diboride (ZrB_2) and hafnium diboride (HfB_2) exhibit high melting points (> 3000 °C) coupled with low theoretical densities, high electrical conductivities, good chemical inertness and excellent wear resistance. Thus, they are expected to be leading candidate materials for the future high-temperature structural applications in aerospace, refractory materials in foundries and electrical devices [28].

ZrB_2 -SiC composite can be healed completely only in an air environment. Therefore, it is assumed that the crack-healing ability is due to oxidation in air. ZrB_2 is preferentially oxidized to ZrO_2 and B_2O_3 according to reaction (12) below when exposed to oxidizing environments at temperatures of about 800 °C.



Due to its low melting temperature (~ 450 °C), the B_2O_3 layer can seal the surface and present an effective barrier to the transport of oxygen, leading to passive oxidation behavior with parabolic weight gain kinetics [29]. With the increasing temperature, SiC oxidizes to form a silica-rich layer (reaction (13)). This layer, namely

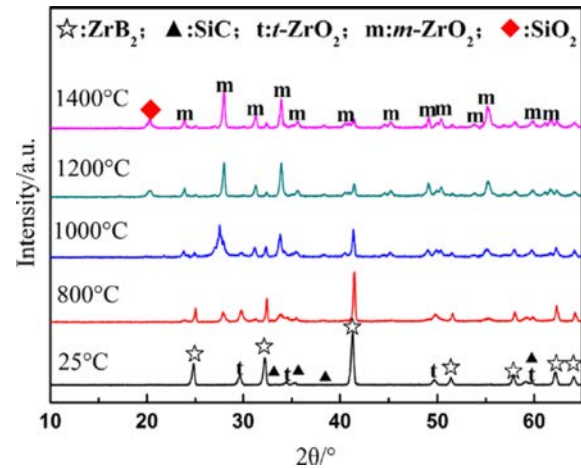


Fig. 18. XRD patterns of the oxide scales on the ZrB_2 -SiC- ZrO_2f substrate after crack-healing at 800-1400 °C for 30 min. From [32].

borosilicate glass layer, afforded more protection than the B_2O_3 layer due to its higher melting temperature and lower vapor pressure. At the same time, it can heal the surface flaws and play a significant role in strength recovery after crack-healing [30].

In case of ZrB_2 -SiC- ZrO_2 composite, ceramic has an excellent combination of properties, such as high fracture toughness ($8.0 \pm 0.5 \text{ MPam}^{0.5}$) and flexural strength ($680 \pm 45 \text{ MPa}$) [31]. Fig. 18 shows the XRD patterns of the oxide scales on the ZrB_2 -SiC- ZrO_2f samples after crack healing at 800-1400 ± for 30 min, compared with the as-received specimens. ZrB_2 as the main phase accompanied with small amount of SiC and tetragonal ZrO_2 (t- ZrO_2) are detected for the sample recorded at room temperature. At 800 ±, a broadened diffraction peak appears at around $2\theta = 28^\circ$, which corresponds well to the monoclinic ZrO_2 (m- ZrO_2) (111) peak.

The new phases are formed through the reaction (12). The new formed t- ZrO_2 phase in the oxide scales would transform to m- ZrO_2 during cooling process. Moreover, no B_2O_3 is detected in the oxide scales due to volatilization. The remaining B_2O_3 is non-crystalline phases and contribute to healing the pre-cracks. With increasing temperature, the diffraction peaks of m- ZrO_2 get sharper and the absolute intensity also increases, which is mainly caused by the increase in the thickness of the oxide layer. At 1000 °C, it can be observed that significant change has taken place in the phase compositions, since the original phases, ZrB_2 , t- ZrO_2 and SiC have decreased and the main phase has become to the m- ZrO_2 phase. Moreover, few weak diffraction peaks for the substrate are seen at the temperature of 1200 °C, indicating that ZrB_2 -SiC- ZrO_2f suffers serious oxidation, while the intensity of the diffraction peaks associated with m- ZrO_2 increases greatly and a new compound, SiO_2 is formed. Based on these observations it can be concluded that SiC begins

to oxidize to SiO_2 and CO at 1200°C according to reaction (13). At 1400°C , the diffraction peaks of SiO_2 become sharper, indicating the growth of crystalline.

Self-healing Parameters

Healing Temperature

Crack-healing behavior is very sensitive to crack-healing temperature. A crack-healing behavior was investigated on the alumina-based composite. Fig. 19 shows flexural strength values for pre-cracked and healed specimens. For the healed specimens at temperature of 1300°C is evident that reference values of σ_0 smooth (unflawed) specimens have been successfully reached and fracture origin was out of pre-cracked zone (full symbols). Therefore these healing conditions seem to be the optimal. The maximal value of flexural strength for pre-cracked specimens (Vickers 20 N) was about 250 MPa, at the same time, maximal flexural strength of pre-cracked and healed specimen reached more than 1000 MPa. There is an indication that by application of appropriate reactant before healing on the surface can be lowered either healing temperature or healing time. Results of application of oxidizing agent are shown in Fig. 20 by grey symbols and grey dashed line illustrates the maximal reached effect up to now.

Same as alumina monolith and alumina-SiC composite material was compared temperature dependence. The relationship between the crack-healing temperature and the bending strength are shown in Fig. 24. The bending strength of the smooth specimens was 255 MPa and 440 MPa, respectively. The bending strength of heat treated smooth specimens was about 370 MPa and 600 MPa, respectively. The cracked specimens were 230 MPa and 220 MPa. The open circle symbol and solid circle symbol show that of the specimen crack healed from 1373 K to 1723 K. The bending strength of crack-healed specimen, below 1573 K was similar to that of the cracked specimen, indicating that crack-healing was incomplete. The bending strength of crack-healed specimen at 1723 K shows about 280 MPa higher than 255 MPa of smooth specimen. All specimens recovered bending strength, and showed that the cracks were healed completely.

Another case of zirconium dioxide and silicon carbide composite, the effect of crack-healing temperature on the flexural strength of crack-healed specimens at room temperature was investigated. The test results are shown in Fig. 21. The average flexural strength of crack-healing specimens are ~ 699 MPa (800°C , 1 h), 889 MPa (1000°C , 1 h) and 797 MPa (1200°C , 1 h), all higher than that of cracked samples (279 MPa). Moreover, the strength at 1000°C for 1 h shows a 90 MPa increase compare to that of the polished specimens. These results suggest that $\text{ZrB}_2\text{-SiC}$ composite has good self-crack-healing ability in the studied temperature range, and

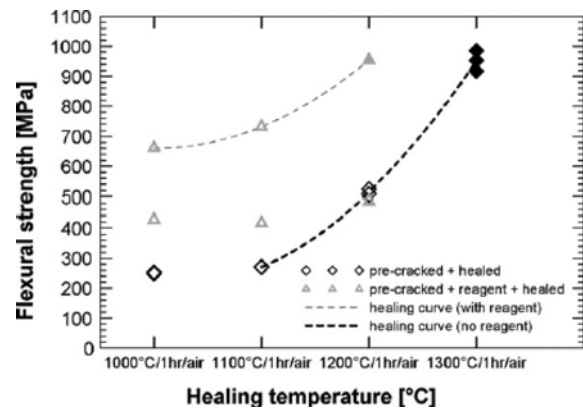


Fig. 19. Dependence of flexural strength of the pre-cracked specimens by Vickers indenter (load 20 N) on healing temperature for the composite. From [9].

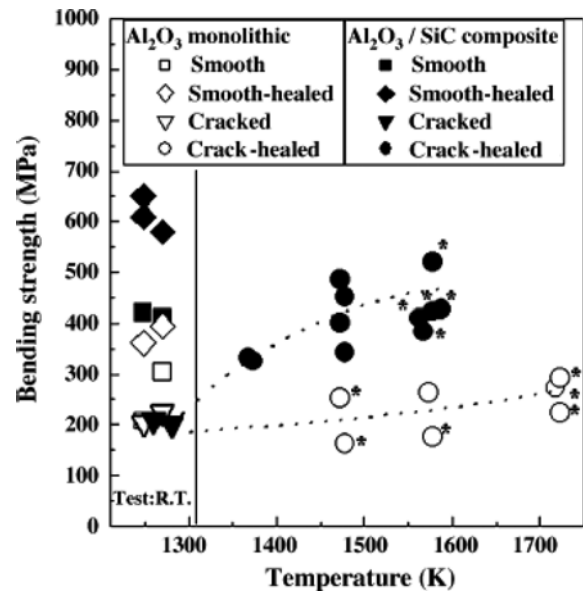


Fig. 20. Relation between the crack-healing temperature and the bending strength at room temperature. From [33].

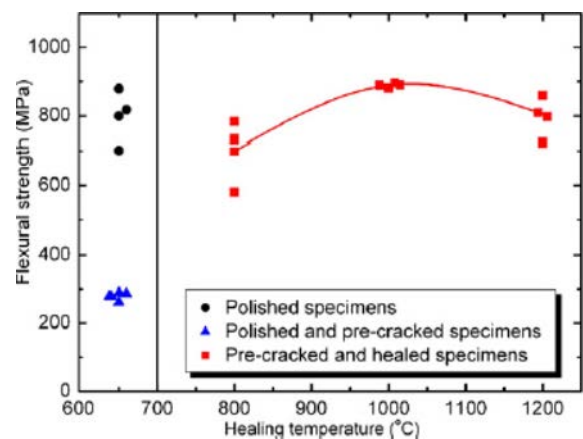


Fig. 21. Effect of crack-healing temperature on the crack-healing behavior. From [30].

that 1000°C is the optimum crack-healing temperature.

Similarly, $\text{ZrB}_2\text{-SiC- ZrO}_2$ has optimum temperature.

The average flexural strength of crack-healing specimens are 556 ± 33 MPa (800 °C, 30 min), 604 ± 45 MPa (1000 °C, 30 min), 775 ± 22 MPa (1200 °C, 30 min) and 621 ± 19 MPa (1400 °C, 30 min), all higher than that of cracked samples (319 ± 10 MPa). Moreover, the strength at 1200 °C for 30 min shows a ~ 95 MPa increase compared to that of the polished specimens. According to the results of SEM and XRD analysis, ZrB_2 is preferentially oxidized to form ZrO_2 particles which would fill in the crack gaps for temperature below 1000 °C, and the oxidation products increase with the increasing temperature. This oxidation layer enables the cracked specimens to recover their strength to the same level of the polished samples. Then, when the temperature is up to 1200 °C, a dense oxide layer, contained ZrO_2 and SiO_2 , can easily heal the Vickers indentation and cracks, thus exhibiting the optimum strength recovery performance. As the oxidation temperature up to 1400 °C, the oxide layer becomes thicker. As known, the strength of oxide layer is lower than the matrix ceramic, so the strength of ZrB_2 -SiCw- ZrO_2 f ceramic oxidized at 1400 °C would decrease as shown in Fig. 22 when the oxide layer is too thick. The key to utilize the surface oxidation for crack-healing is that the thickness of oxidation must be enough for crack-healing but not too much to decrease its mechanical properties.

The temperature range at which self-crack-healing is valid is limited by the crack-healing rate and the high temperature properties. Assuming that fracture by the damage allows complete healing of surface cracks introduced by first damage in 100 h, one can evaluate the valid temperature range of the self-crack-healing as listed table 4.

Testing Temperature

Fig. 23 shows the effect of test temperature on the σ_B of crack-healed structural ceramics developed by K. Ando *et al* [19, 40-43]. The phase of grain boundary and crack-healed zone of Si_3N_4 exhibited the glassy phase, thus the bending strength decreased suddenly over 1273 K [40]. On the other hand, the Si_3N_4/SiC exhibited the crystal phase in both areas, thus it exhibited very high limiting temperature for bending strength (1573 K) [41]. The Al_2O_3/SiC exhibited a very high limiting temperature for bending strength (1573 K) compared to that of monolithic Al_2O_3 , because very small SiC particles (0.27 μm) were distributed in Al_2O_3 grain and formed nano-size composite material [43]. The mullite/SiC also exhibited quite a high limiting temperature for bending strength (1523 K) [19]. Recently, the SiC for which the crack-healed zone exhibited high limiting temperature for bending strength (≈ 1573 K) was developed [39].

The temperature limit is affected by the fractures of the oxide formed by self-crack-healing. The commercial sintered SiC was found considerably low temperature

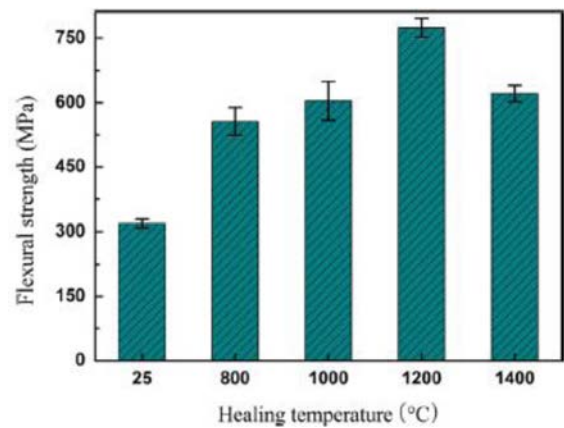


Fig. 22. Effect of crack-healing temperature on the flexural strength of the composite. From [32].

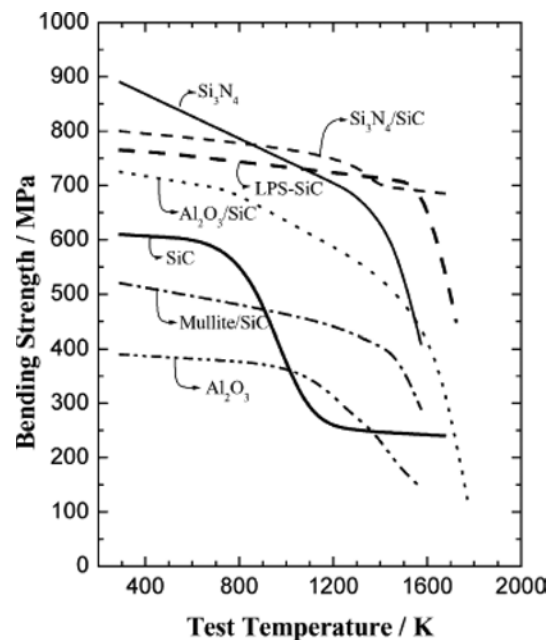


Fig. 23. Effect of testing temperature on the bending strength of crack-healed structural ceramics. From [16].

limit of 873 K because the formed SiC is in glassy phase [15]. Modifying the sintered additives to Sc_2O_3 and AlN, the temperature limit succeeded in improving of the cracked zone significantly [39]. When the sintered additive is 5 wt% Y_2O_3 and 3 wt% Al_2O_3 , the formed oxide and grain boundary are in glassy phase. Alternatively $Si_3N_4/20$ wt% SiC particles composite containing 8 wt% Y_2O_3 as sintering additives forms the crystalline oxide, such as $Y_2Si_2O_7$ by crack-healing. Alumina/15 vol% SiC particles composite and mullite/15 vol% SiC particles composite form crystalline phase because the formed oxide reacts with the matrix and formed mullite (reaction (11)). Temperature limit are summarized in Table 5.

Healing time

Crack-healing behavior is sensitive to crack healing time at certain temperature. Fig. 24 shows the

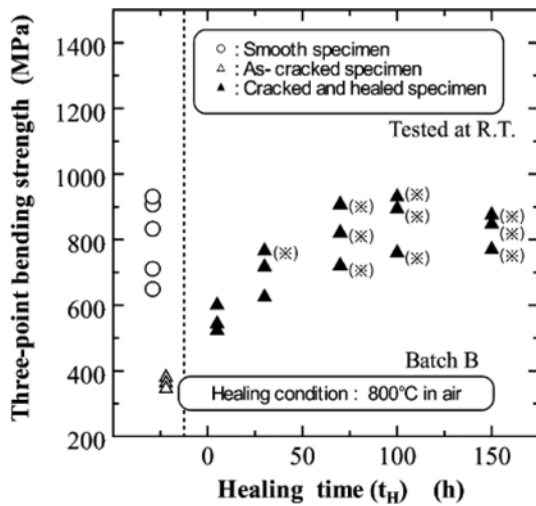


Fig. 24. Relationship between healing time and bending strength of Si₃N₄/SiC ceramics at room temperature. Data with an asterisk indicates that fracture occurred outside of the crack-healed zone. From [34].

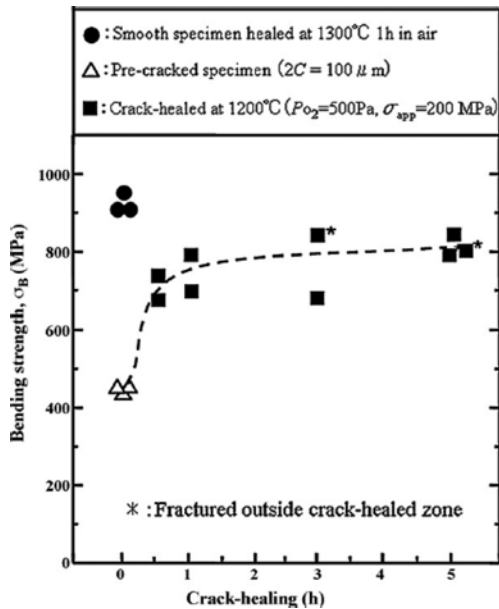


Fig. 25. Relationship between bending strength at room temperature and crack-healing time at 1200 °C under tensile stress of 200 MPa in PO₂ = 500 Pa. From [35].

relationship between bending strength at room temperature and crack-healing time for Si₃N₄-SiC. The specimens with a surface crack (2c = 100 μm) were crack-healed at 800 °C in air. Bending strength of the crack-healed specimen recovered if the crack-healing time was longer than 70 h. However, whether the crack-healed specimens have enough strength at 800 °C is not studied yet.

Similarly, as of Si₃N₄-SiC composite ceramic, Fig. 25 shows the relationship between the bending strength at room temperature and the crack-healing time at 1200°C under a tensile stress (σ_{app}) of 200 MPa in PO₂ = 500 Pa. The applied stress of 200 MPa was 45% of the bending strength of the pre-cracked specimens. The

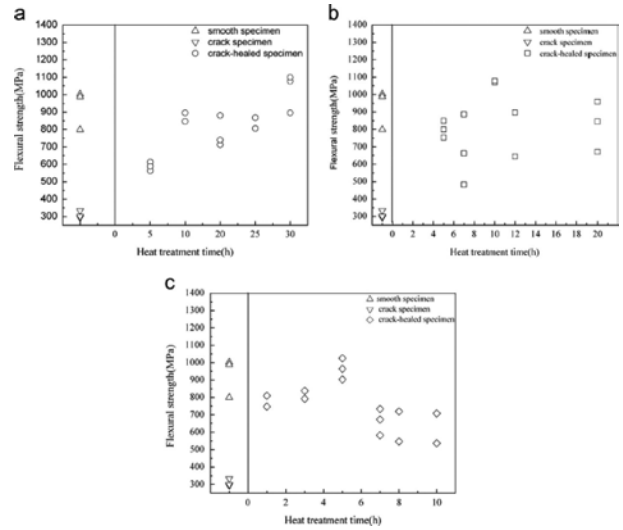


Fig. 26. Variations of flexural strength of TZ3Y20A-SiC ceramics as a function of heat treatment time at different temperatures: (a) 800 °C; (b) 1000 °C; and (c) 1100 °C. From [38].

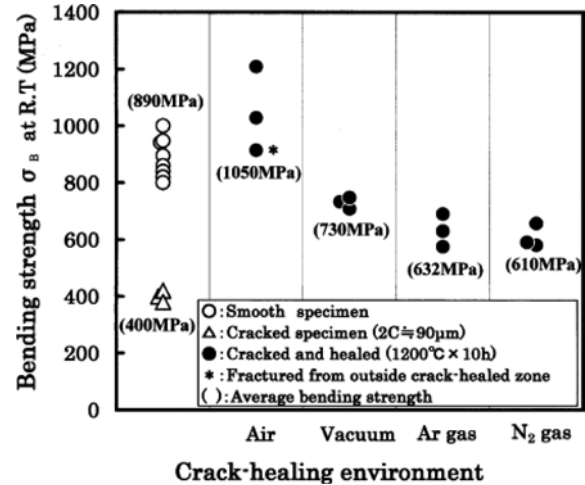


Fig. 27. Effect of crack-healing environment on the strength recovery behavior. From [17].

solid circles indicate the bending strength (σ_B) of the smooth specimen healed at 1300 °C for 1 h in air. The open triangles indicate the bending strength of the pre-cracked specimens. The average bending strength of the smooth specimens was 930 MPa, and that of the pre-cracked specimens was 440 MPa. The bending strength of the pre-cracked specimens decreased by 53% due to the pre-cracks that introduced by the Vickers indentation. The solid square symbols indicate the bending strengths of the crack-healed specimens which crack-healed at 1200 °C under a stress of 200 MPa in PO₂ = 500 Pa. In the specimens with asterisks, fracturing occurred outside of the crack-healed zone as shown in Fig. 26, which indicated that the pre-crack was healed completely. For the 1 h crack-healing treatment, the bending strengths increased up to about 720 MPa, but this did not represent complete strength recovery. On the other hand, for the 5h crack-healing

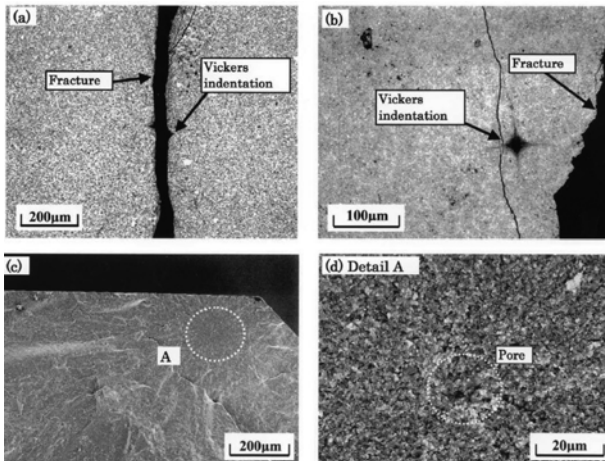


Fig. 28. Fracture pattern of crack-healed sample: (a) crack initiated from crack-healed zone, TH = 900 °C, tH=100h, σ_B = 896 MPa, (b) crack initiated from the outside of crack-healed zone, TH = 1100 °C, tH = 100 h, σ_B = 889 MPa, (c) fracture surface of sample (b), (d) in detail of (c). From [17].

treatment, the crack-healed specimens significantly recovered their strength, to a value of about 850 MPa. By means of the crack-healing at 1200 °C for 5 h, the crack-healed specimen showed almost the same strength as the healed smooth specimen. Moreover, the fracturing in two specimens occurred outside the crack-healed zone. Therefore, it was confirmed that complete strength recovery could be achieved under tensile stress in low oxygen partial pressure conditions ($\sigma_{app.} = 200$ MPa, $PO_2 = 500$ Pa) by crack-healing at 1200 °C for 5 h.

After heat treatments of $TZ_3Y_{20}A$ -SiC ceramics at different temperatures, flexural strength are higher than those of smooth specimens. In consideration of flexural strength recovery and crack-healing results, the optimized heat treatment time required for complete crack-healing effect at temperatures of 800 °C, 1000 °C, 1100 °C and 30 h, 10 h, and 5 h, respectively. The oxidized products of β -SiC include two phases of a glassy phase and a crystalline SiO_2 . The glass phase that form at relatively low temperature or short healing time during heat treatment contributes to the healing of pre-cracks [35]. However, excess crack-healing time over the optimum condition will cause the performance degradation. The glassy phase transforms to the crystalline phase α - SiO_2 , and then partial crystalline α - SiO_2 reacts with Y_2O_3 to generate gamma- $Y_2Si_2O_7$ with further enhancing temperature or increasing the healing time during heat treatment [36]. These oxidized products fill up into the cracks to provide a sufficient strength recovery of $TZ_3Y_{20}A$ -SiC ceramics.

Healing atmosphere

In case of Si_3N_4/SiC ceramics, Fig. 27 shows the bending strength (σ_B) of specimens healed in each environment. The contrast between σ_B of smooth

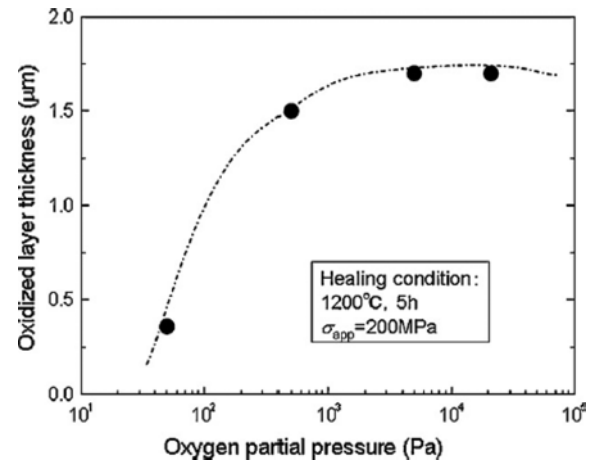


Fig. 29. Relationship between oxidation layer thickness and oxygen partial pressure. From [35].

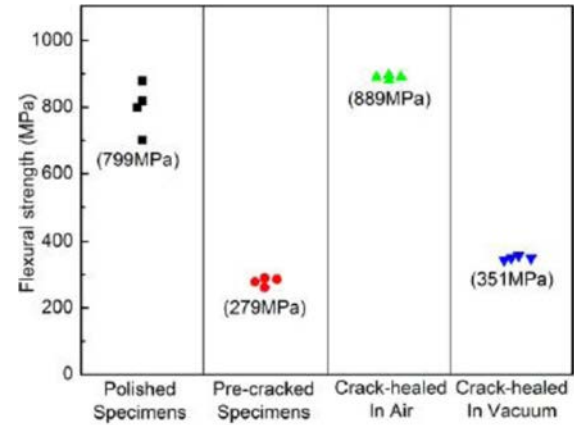


Fig. 30. Effect of pre-cracking and crack-healing environment on the flexural strength of the composite, From [30].

specimens (*) and cracked specimens (Δ) is shown by the left-most column of result. The symbol (*) indicates a specimen that fractured outside the crack-healed zone as shown in Fig. 28(b). All samples healed in air recovered σ_B completely, and showed that the cracks were healed completely.

One sample fractured from outside the crack-healed zone as shown in Fig. 28(b). Fig. 28(c) and (d) show the crack initiation site of Fig. 28(b). Fracture initiated from a small pore.

Specimens healed in vacuum, Ar gas and N_2 gas indicated that the strength recovery was insufficient, and all samples fractured from the crack healed zone as shown in Fig. 28(a). The average σ_B of the specimens healed in vacuum is 730 MPa, which is a little higher than that of the other two conditions (Ar gas and N_2 gas). Therefore, it is assumed that the crack-healing is due to oxidation.

Similarly, Si_3N_4/SiC ceramics, the oxidized layer thicknesses were analyzed based on fracture surface observation using SEM, after crack-healing at 1200 °C for 5 h, as a function of oxygen partial pressure. Fig.

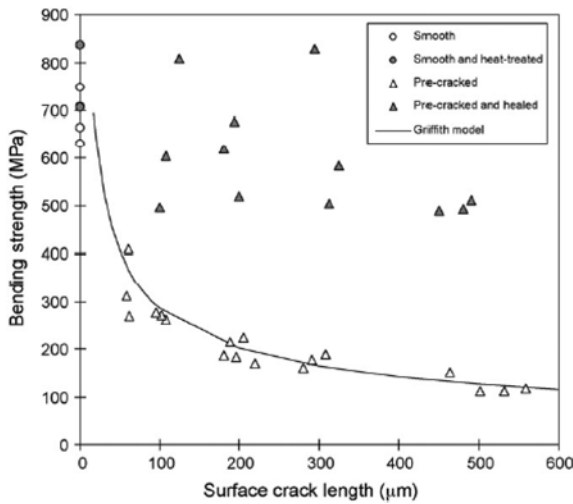


Fig. 31. Bending strength of pre-cracked specimens with or without crack healing as a function of surface length of pre-cracks (healing condition: 1300 °C, 1 h in air). From [45].

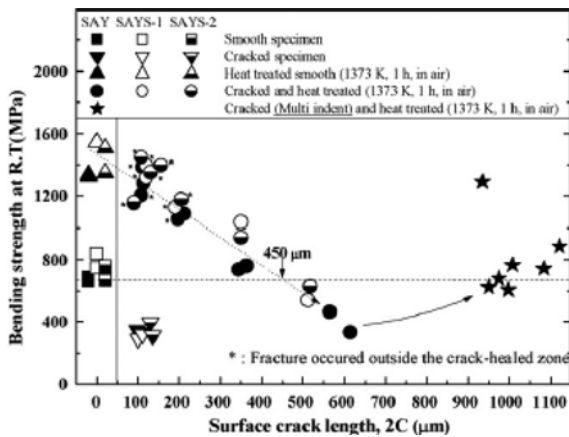


Fig. 32. Effect of pre-crack length on the bending strength for crack-healed specimens, From [46].

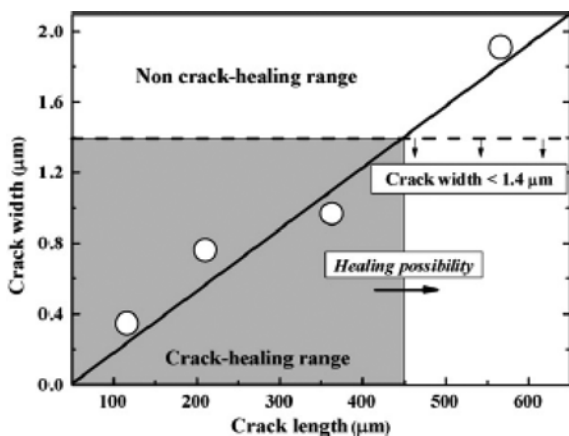


Fig. 33. Relationship between surface crack length and crack width of healing possibility, From [46].

29 shows the relationship between the oxidation partial pressure and the oxidized layer thickness. The oxidized layer thickness of the crack-healed specimens in $PO_2 = 50$ Pa was about $0.3 \mu\text{m}$. This indicates that the

oxidation reactions occurred in the surface area, but were not sufficient to heal the cracks. The crack opening size was about $0.2\text{--}0.3 \mu\text{m}$, and the depth was about $40\text{--}50 \mu\text{m}$. Therefore, greater heat generation at a higher temperature or for a longer time would be required to heal the crack completely. On the other hand, the oxidized layer thickness was significantly increased by crack-healing in $PO_2 \geq 500$ Pa. The thickness was about $1.7 \mu\text{m}$. By means of the formation of an oxidation layer, the cracks were completely filled with oxidation products, and the strengths were completely recovered.

The presence of oxygen causes the self-healing phenomenon, as crack-healing driven by the oxidation of SiC. The ZrB_2/SiC ceramics, as shown in Fig. 30, all samples healed in air recovered a good flexural strength relative to that of polished specimens, indicating that the cracks could heal completely. However, specimens treated in vacuum under the same healing conditions (temperature and time are 1000°C and 1 h, respectively) showed that the strength recovery was insufficient. The average flexural strength of vacuum-healed samples was 351 MPa, which was a little higher than the value of cracked specimens. This slight increase in strength was probably caused by the removal of residual stress ahead of the cracks [16]. Crack-healing in vacuum did not change the fracture pattern of specimens and all samples also fractured from the Vickers indentation zone. This may be another reason for the insufficient strength recovery in vacuum.

Crack Size

In the case of the SiC-AlN composites, results of the bending strength of pre-cracked specimens with or without crack-healing as a function of surface length of pre-cracks are reported in Fig. 35. In this graph the open circle and solid circle indicate smooth specimens without or with heat-treatment at 1300°C for 1 h in air. The open triangles indicate the pre-cracked specimens, as the surface length of the pre-crack increased, the bending strength decreased. The solid triangles indicate the bending strength of crack-healed specimens. The specimens subjected to crack-healing at 1300°C showed an increase of the bending strength.

The experimental results indicated that large cracks up to about $300 \mu\text{m}$ could be completely healed at 1300°C . In fact, the cracks of this length are completely closed at this temperature and the increased strength was due to a substantial increase in the bonding force acting across the crack surfaces as a consequence of the formation of the oxidation products. Furthermore, the dashed line reported in Fig. 31 demonstrates that the bending strength values obtained with the pre-cracked samples obey to the Griffith model:

$$\sigma_B = \frac{K_{IC}}{F\sqrt{\pi a}} \tag{14}$$

Where σ_B is the bending strength, K_{IC} is the fracture

toughness ($3.5 \text{ MPam}^{0.5}$ determined by indentation fracture method), F is the geometry factor (0.69 for semi-elliptical surface crack with aspect ratio $a/c = 0.9$) [44] and a is the half length of the surface crack.

In the other case of $\text{SiC-Al}_2\text{O}_3\text{-Y}_2\text{O}_3\text{-SiO}_2$ ceramics, the dependence of strength on the surface crack size ($2c$) for crack-healing behavior is shown in Fig. 32. The strengths of the cracked specimens were half of that of the smooth specimens. The strengths of the cracked specimens where healing took place decreased linearly as the surface crack length increased.

The crack-healed specimens exhibited higher strength than the smooth specimens when the crack length was $\leq 350 \mu\text{m}$. Although specimens were fractured at the crack-healed part at a crack length of $2c = 350 \mu\text{m}$, they nevertheless displayed a good strength property. The sintering additive for the limit length of crack-healing had nothing to do with the type of SiO_2 employed. That is, all specimens were likely to be healed within a crack length of $2c = 450 \mu\text{m}$, by using $\text{SiC-Al}_2\text{O}_3\text{-Y}_2\text{O}_3\text{-SiO}_2$ ceramics, the relationship between crack length and crack width shows at Fig. 33. As the Vickers indentation load increased, crack length and crack width also increased linearly. The surface crack length of the crack-healing possibility was about $2c = 450 \mu\text{m}$. The crack width at that time was about $1.4 \mu\text{m}$. These results show that the critical size of crack-healing possibility, which indicates that crack width is very important to crack healing. That is, if the crack width is below $1.4 \mu\text{m}$, the material is likely to heal even if crack length is above $450 \mu\text{m}$.

SiC volume fraction

SiC volume Fig. 34 shows the experimental results. The crack introduced on the test specimen is a semi-elliptical crack $100 \mu\text{m}$ in surface length and $45 \mu\text{m}$ in depth (hereafter called a standard crack). The open circles show the fracture of the specimens initiated from outside the crack-healed zone, indicating that complete crack healing occurred. With respect to strength, the optimal volume fraction of SiC is 7.5% to 10%. There are two kind of fracture mode. One is the fracture initiated from the crack-healed zone that formed oxide is not enough to heal the pre-crack completely. The other is the fracture initiated outside the crack-healed zone that formed oxide is enough to heal the crack. Considering crack-healing ability, a volume fraction of SiC larger than 10% is recommended. However, when the SiC additive rate exceeds 30%, the strength begins to vary greatly, since a SiC agglomeration is formed. On the other hand, a large crack can be healed with an increased SiC volume fraction. The authors recommend a standard SiC volume fraction of 15~30%. Crack-healing report can have three generations based on the SiC volume fraction, Table 13.

Applied healing and testing stress

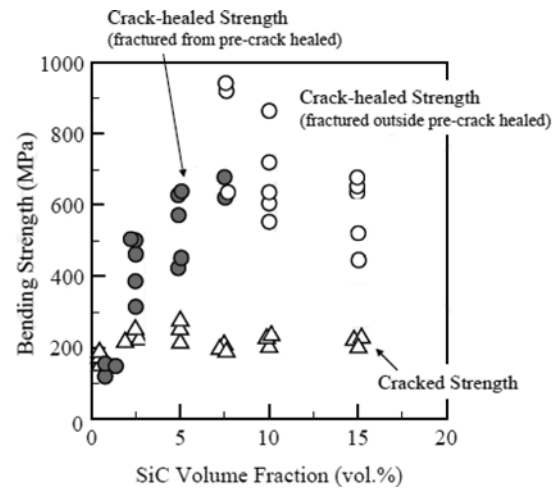


Fig. 34. Crack-healed and cracked strength of a $\text{Al}_2\text{O}_3/\text{SiC}$ composites as a function of SiC volume fraction, From [47].

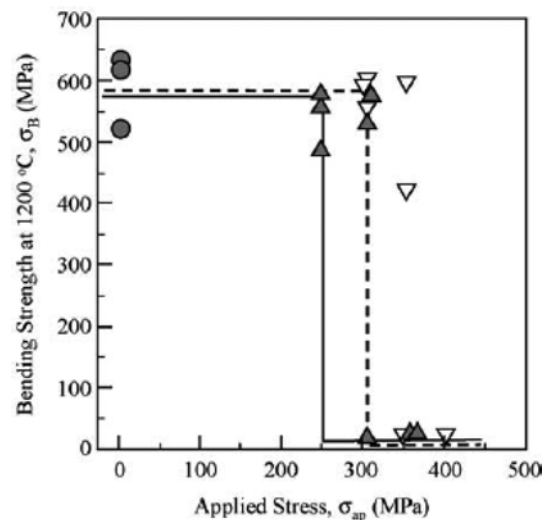


Fig. 35. Relation between the applied stress during the crack-healing treatment for the specimens as-cracked and the bending strength at the crack-healing temperature of the specimens crack-healed under static and cyclic stress. (\blacktriangle) Crack-healed under static stress; (∇) crack-healed under cyclic stress; (\bullet) crack-healed under no stress. From [48].

Alumina reinforced by SiC whisker, alumina (w) was developed with the objective of improving fracture toughness and crack-healing ability. The composites were crack-healed at $1200 \text{ }^\circ\text{C}$ for 8 h in air under elevated static and cyclic stresses and the bending strength at $1200 \text{ }^\circ\text{C}$ of the crack healed composites were then investigated in Fig. 35. Alumina (w) with the pre-crack of $100 \mu\text{m}$ were never fractured during crack-healing treatment under static stresses below 250 MPa , and the crack-healed specimen had the same bending strength as the specimens crack-healed under no-stress at $1200 \text{ }^\circ\text{C}$. Therefore, the threshold static stress during crack-healing of alumina (w) was found to be 250 MPa . Also, the threshold cyclic stress was found to be 300 MPa . Considering that the crack growth is time-dependent, the threshold stress of every

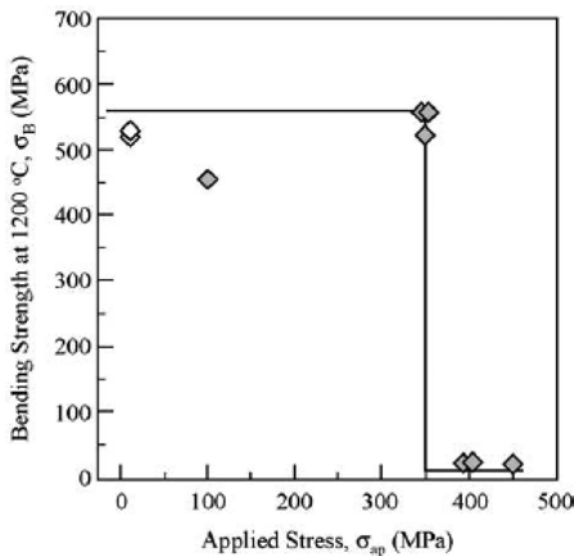


Fig. 36. Relation between the applied stresses during the crack-healing treatment for the specimen annealed after pre-cracking and the bending strength at the crack-healing temperature of the specimens crack-healed under static stress. (\blacklozenge) Crack-healed under static stress; (\diamond) crack-healed under no stress. From [48].

condition during crack-healing of alumina (w) has been concluded to be 250 MPa.

Moreover, the same experiment is conducted on specimens annealed at 1300 °C for 1 h in Ar after pre-cracking. Thus, the threshold static stress during crack-healing of alumina (w) annealed after pre-cracking has been determined to be 350 MPa in Fig. 36. From the results, the threshold stress intensity factor during crack-healing has been evaluated as 3.8 and 3.2 $\text{MPam}^{0.5}$ for the specimen crack healed without annealing and with annealing, respectively. A comparison with the values of the threshold stress intensity factor during crack-healing shows that the residual stress is slightly larger than the intrinsic value. Therefore, the threshold stress intensity factor during crack-healing of alumina (w) is selected as 3.2 $\text{MPam}^{0.5}$.

Threshold stress for crack-healing

The crack-healing occurs although the pre-crack is grown by the applied stress. Alumina/15 vol% SiC particle composite and mullite/15 vol% SiC particles composite, that have excellent crack-healing ability are subjected to crack-healing under elevated static and cyclic stresses at 1373 K or 1473 K in Fig. 37. The bending strengths of the specimens crack-healed under stress were investigated at the crack-healing temperature. From the result, the threshold stresses during crack-healing were determined. The threshold static and cyclic stresses during crack-healing for alumina/15 vol% SiC particle composite were found to be 150 MPa and 180 MPa, respectively. Also the stresses for mullite/15 vol% SiC particles composite were found to be 115 MPa and 125 MPa, respectively. It is found that crack-healing

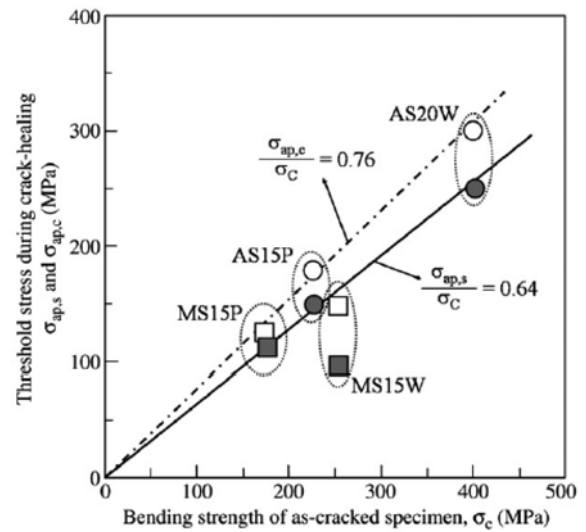


Fig. 37. Threshold static and cyclic stresses during crack-healing as a function of the fracture strength for the corresponding as-cracked specimens, in which the closed and open symbols indicate the data of the threshold static and cyclic stresses, respectively. From [49].

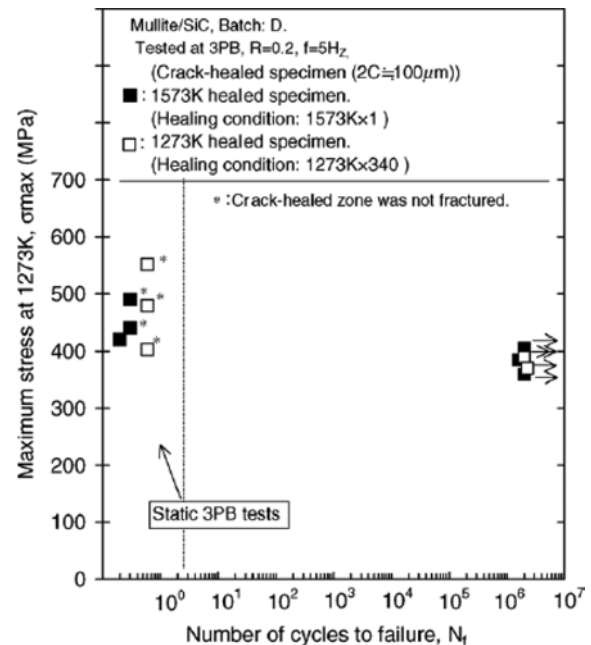


Fig. 38. Effect of crack-healing temperature on the fatigue strength of mullite/SiC, From [50].

can eliminate the pre-crack under stress below 64% σ_c , if the ceramic components have an adequate crack-healing ability. The proportional constants for the relationship between the threshold stress and bending strength of pre-cracked specimens is 64% for constant stress and 76% for cyclic stress.

Fatigue strength

The effect of self-crack healing on the fatigue strength is greater than that of the monotonic strength. The fatigue degradation of ceramics progresses by the stress

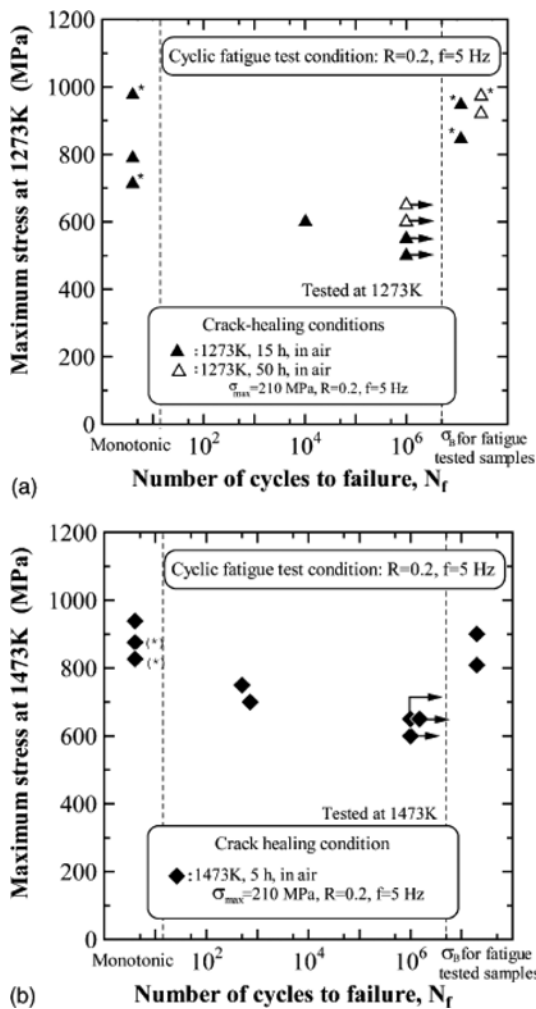


Fig. 39. Cyclic fatigue strength of crack-healed Si₃N₄ at the crack-healing temperature of 1273 and 1473 K. Data marked with an asterisk indicate that fracture occurred outside of the crack-healed zone.

corrosion cracking at the tip of the crack. Therefore, the presence of surface cracks affects strongly the fatigue strength. The cyclic fatigue strength of mullite/SiC at 1273 K was shown in Fig. 38. The symbols (■) and (□) indicate that the standard cracks of mullite/SiC were healed at 1573 K, 1h, and 1273 K, 340 h, respectively. Both samples showed the same fatigue limit (400 MPa). From this test results, it can be concluded that the mullite/SiC exhibits excellent in situ crack-healing ability even for fatigue strength.

The cyclic fatigue strength of Si₃N₄/SiC at 1273 K and 1473 K was shown in Fig. 39, that were crack-healed under the cyclic stress at 1273 K and 1473 K, respectively [14]. The crack healed under the very severe condition (5 Hz cyclic stress of 210 MPa). The stress 210 MPa is the fatigue limit of this sample with $2c = 100$ μ m surface crack at room temperature [50]. At 1273K, the 15 h healed sample exhibited a rather low fatigue limit of 550 MPa, however, the 50h-healed sample exhibited the very high fatigue limit of 650 MPa. At both temperatures, samples crack-healed

under cyclic stress exhibited a high fatigue limit of 650 MPa. Thus, it can be concluded that this Si₃N₄ developed by the authors also exhibits excellent in situ crack-healing ability even under cyclic stress.

Conclusions

Silicon Carbide Ceramics has low thermal expansion coefficient and high thermal conductivity, strength and hardness, make SiC a promising ceramic for the replacement of conventional metals, alloys and ionic bonded ceramic oxides. Machining is a necessary process to meet the complexity of ceramic design, but machining can cause many cracks.

The cracks collected as a brittle of ceramics, which seriously affects the reliability of ceramic components. Four methods are used to resolve this weakness: (a) the ceramic is toughened by fiber reinforcement or microstructural control, (b) high level non-destructive inspection and repair of the unacceptable flaws, (c) using the proof test and then only using the components that have high reliability, and (d) making use of the self-crack-healing ability. In this paper, special attention was paid to method (d), the self-crack-healing ability of structural ceramics.

It is explained in detail how the cracks introduced can be healed and mechanical strength recovered completely. If a material were able to heal a crack that initiated during its service, it would be extremely beneficial for the structural integrity of a ceramic component. Even if all surface cracks were healed completely, embedded flaws such as cracks and pores cannot be healed that cause unexpected failure. The crack-healing behavior under stress and the resultant strength at the crack-healing condition are important to understand actual usage of ceramic.

In conclusion, the crack-healing ability of structural ceramics is a very useful technology for higher structural integrity and for reducing the machining and non-destructive inspection costs.

For the further studies, we need investigate self-healing behavior not only mechanical properties but also thermal and electrical performance consistency to extend advanced application.

References

1. R. Riedel (2000) Handbook of Ceramic Hard Material, Wiley-VCH.
2. T. Osada et al (2007) Strength recovery behavior of machined Al₂O₃/SiC nano-composite ceramics by crack-healing. J Eur Ceram Soc 27:3261-3267.
3. Z. Chlup et al (2008) Fracture behaviour of Al₂O₃/SiC nanocomposite ceramics after crack healing treatment. J Euro Ceram Soc 28:1073-1077.
4. K. Houjou et al (2004) Crack-healing and oxidation behavior of silicon nitride ceramics. J Eur Ceram Soc 24:2329-2338.
5. K.W. Nam et al (2007) Crack-healing behavior and bending

- strength of Si₃N₄/SiC composite ceramics by SiO₂ colloidal. *Materials Science and Engineering A* 471:102-105.
6. W.D. Kingery et al (1976) *Introduction to Ceramics*, 2nd edn. Wiley, New York, p. 63.
 7. X.-P. Zhangetal(2014) Crack-healing behavior of hot-pressed TZ3Y20A-SiC ceramics. *Ceramics International* 40:6611-6615.
 8. K. Ando et al (2002) Crack healing behaviour and high-temperature strength of mullite/SiC composite ceramics. *J Eur Ceram Soc* 22:1313-1319.
 9. Cartwright Morgan Advanced Materials have weather too, <http://www.morgantechnicalceramics.com/materials/zirconia-zro2>. Accessed at Nov. 2014.
 10. K. Ando et al (2002) Crack-Healing Behavior of Si₃N₄/SiC Ceramics under Cyclic Stress and Resultant Fatigue Strength at the Healing Temperature. *J Am Ceram Soc* 85:2268-2272.
 11. S.-P. Liu et al (2009) In situ crack-healing behavior of Al₂O₃/SiC composite ceramics under static fatigue strength. *Int Commun Heat Mass* 36:563-568.
 12. S. K. Lee et al (2005) Crack-healing behavior and resultant strength properties of silicon carbide ceramic. *J Eur Ceram Soc* 25:569-576.
 13. K. Houjou et al (2004) Crack-healing and oxidation behavior of silicon nitride ceramics. *J Eur Ceram Soc* 24:2329-2338.
 14. F. Yao et al (2000) Crack-healing behavior, high temperature and fatigue strength of SiC-reinforced silicon nitride composite. *J Mater Sci Lett* 12:1081-1083.
 15. K. Ando et al (2002) Crack healing behaviour and high-temperature strength of mullite/SiC composite ceramics. *J Eur Ceram Soc* 22:1313-1319.
 16. S.R. Choi, V. Tikare (1992) Crack healing behavior of hot pressed silicon nitride due to oxidation. *Scripta Metall Mater* 26:1263-1268.
 17. K. Ando et al (2003) Effect of crack-healing and proof-testing procedures on fatigue strength and reliability of Si₃N₄/SiC composites. *J Eur Ceram Soc* 23:977-984.
 18. T.K. Gupta et al (1976) Crack Healing and Strengthening of Thermally Shocked Alumina. *J Am Ceram Soc* 59:259-262.
 19. H.W. Kim et al(1999) Effect of Oxidation on the Room-Temperature Flexural Strength of Reaction-Bonded Silicon Carbides. *J Am Ceram Soc* 82:1601-1604.
 20. B.S. Kim et al (2003) Crack-Healing Behavior of Monolithic Alumina and Strength of Crack-Healed Member. *J Soc Mater Sci Japan* 52:667-673.
 21. S.P. Liu et al (2009) In situ crack-healing behavior of Al₂O₃/SiC composite ceramics under cyclic-fatigue strength. *Int. Commun. Heat Mass Tran* 36:558-562.
 22. G. Magnani et al (2006) Long term oxidation behaviour of liquid phase pressureless sintered SiC-AlN ceramics obtained without powder bed. *J Eur Ceram Soc* 26:3407-3413.
 23. Y. W. Kim et al (2002) Crack-Healing Behavior of Liquid-Phase-Sintered Silicon Carbide Ceramics. *J Am Ceram Soc* 86:465-470.
 24. M.M. Opeka et al (2004) Oxidation-based materials selection for 2000 °C + hypersonic aerosurfaces: Theoretical considerations and historical experience. *J Mater Sci* 39:5887.
 25. F. Monteverde, A. Bellosi (2003) Oxidation of ZrB₂-Based Ceramics in Dry Air. *J Electrochem Soc* 150:552-559.
 26. X. Zhang et al (2008) Crack-healing behavior of zirconium diboride composite reinforced with silicon carbide whiskers. *Scripta Materialia* 59:1222-1225.
 27. J. Lin et al (2012) The hybrid effect of SiC whisker coupled with ZrO₂ fiber on microstructure and mechanical properties of ZrB₂-based ceramics. *Mater. Sci. Eng. A* 551:187-191.
 28. J. Lin et al (2014) Crack healing and strengthening of SiC whisker and ZrO₂ fiber reinforced ZrB₂ ceramics. *Ceramics International* 40:16811-16815.
 29. H.S. Kim et al (2008) Bending strength and crack-healing behavior of Al₂O₃/SiC composites ceramics. *Mat Sci Eng A* 483-484:672-675.
 30. K. Takahashi et al (2003) Crack-healing behavior and static fatigue strength of Si₃N₄/SiC ceramics held under stress at temperature (800, 900, 1000 °C). *J Eur Ceram Soc* 23:1971-1978.
 31. K. Takahashi et al (2010) Crack-healing behavior of Si₃N₄/SiC composite under stress and low oxygen pressure. *Mat Sci Eng A* 527:3343-3348.
 32. Debajyoti Mohanty et al (2011) Development of input output relationships for self-healing Al₂O₃/SiC ceramic composites with Y₂O₃ additive using design of experiments. *Ceram Int* 37:1985-1992.
 33. Kotoji Ando et al (2005) Crack-healing ability of structural ceramics and a new methodology to guarantee the structural integrity using the ability and proof-test. *J Eur Ceram Soc* 25:549-558.
 34. X.-P. Zhang et al (2014) Crack-healing behavior of hot-pressed TZ3Y20A-SiC ceramics. *Ceramics International* 40:6611-6615.
 35. S. K. Lee et al (2005) Effect of Heat Treatments on the Crack-Healing and Static Fatigue Behavior of Silicon Carbide Sintered with Sc₂O₃ and AlN. *J Am Ceram Soc* 88:3478-3482.
 36. Y. W. Kim et al (2003) Crack-Healing Behavior of Liquid-Phase-Sintered Silicon Carbide Ceramics. *J Am Ceram Soc* 86:465-470.
 37. Ando et al (1999) Crack Healing Behavior and High Temperature Strength of Silicon Nitride Ceramics. *J Soc Mech Eng* 65:1132-1139.
 38. F. Yao et al (2001) Static and cyclic fatigue behaviour of crack-healed Si₃N₄/SiC composite ceramics. *J Eur Ceram Soc* 21:991-997.
 39. B. S. Kim et al (2003) Crack-healing behavior of monolithic alumina and strength of crack-healed member. *J Soc Mat Sci Jpn* 52:667-673.
 40. G. Magnani et al (2010) Crack healing in liquid-phase-pressureless-sintered silicon carbide-aluminum nitride composites. *J Eur Ceram Soc* 30:769-773.
 41. Newman Jr. et al (1981) An empirical stress-intensity factor equation for the surface crack. *Eng. Fract. Mech.* 15:185-192.
 42. K.W. Nam, J.S. Kim (2010) Critical crack size of healing possibility of SiC ceramics. *Mat Sci Eng A* 527:3236-3239.
 43. Zwagg, *Self healing Materials*, Springer Verlag, 2007, pp. 183-217.
 44. W. Nakao et al (2005) Critical crack-healing condition for SiC whisker reinforced alumina under stress. *J Eur Ceram Soc* 25:3649-3655.
 45. W. Nakao et al (2007) Threshold stress during crack-healing treatment of structural ceramics having the crack-healing ability. *Materials Letters* 61:2711-2713.
 46. K. Ando et al (2005) Crack-healing ability of structural ceramics and a new methodology to guarantee the structural integrity using the ability and proof-test. *J Eur Ceram Soc* 25:549-558.

47. K. Ando et al (1999) Fatigue strength of crackhealed Si₃N₄/SiC composite ceramics. *FatigueFractEng Mater*

Struct 22:897-903.